THE JOURNAL OF BIOLOGICAL CHEMISTRY VOL. 288, NO. 47, pp. 33824–33836, November 22, 2013

Insulin Secretion and Ca^{2+} Dynamics in β-Cells Are Regulated by PERK (EIF2AK3) in Concert with Calcineurin*

Received for publication, July 22, 2013, and in revised form, October 10, 2013 Published, JBC Papers in Press, October 10, 2013, DOI 10.1074/jbc.M113.503664

Rong Wang[‡], Barbara C. McGrath[‡], Richard F. Kopp[§], Michael W. Roe[§], Xin Tang[‡], Gong Chen[‡], and Douglas R. Cavener[‡1]

From the [‡]Department of Biology, Center of Cellular Dynamics, Pennsylvania State University, Pennsylvania 16802 and the [§]Department of Medicine, Cell and Developmental Biology, SUNY Upstate Medical University, Syracuse, New York 13210

Background: A genetic deficiency in protein kinase R (PKR)-like endoplasmic reticulum kinase (PERK) in human and mice results in insulin-dependent diabetes.
Results: Acute inhibition of PERK impairs insulin secretion, secretagogue-stimulated Ca^{2+} influx, and sarcoplasmic endoplasmic reticulum Ca^{2+}-ATPase activity through a calcineurin-dependent pathway.
Conclusion: PERK and calcineurin regulates Ca^{2+} dynamics underlying insulin secretion.
Significance: Our findings provide insights into the intracellular mechanisms underlying stimulated insulin secretion.

Protein kinase R (PKR)-like endoplasmic reticulum kinase (PERK) (EIF2AK3) is essential for normal development and function of the insulin-secreting β-cell. Although genetic ablation of PERK in β-cells results in permanent neonatal diabetes in humans and mice, the underlying mechanisms remain unclear. Here, we used a newly developed and highly specific inhibitor of PERK to determine the immediate effects of acute ablation of PERK activity. We found that inhibition of PERK in human and rodent β-cells causes a rapid inhibition of secretagogue-stimulated subcellular Ca^{2+} signaling and insulin secretion. These dysfunctions stem from alterations in store-operated Ca^{2+} entry and sarcoplasmic endoplasmic reticulum Ca^{2+}-ATPase activity. We also found that PERK regulates calcineurin, and pharmacological inhibition of calcineurin results in similar defects on stimulus-secretion coupling. Our findings suggest that interplay between calcineurin and PERK regulates β-cell Ca^{2+} signaling and insulin secretion, and that loss of this interaction may have profound implications in insulin secretion defects associated with diabetes.

Insulin secretion from the endocrine pancreatic β-cells is driven by a rapid influx of Ca^{2+} from the extracellular space or from internal stores into the cytoplasm, which stimulates exocytosis of the insulin granules (1, 2). The uptake of Ca^{2+} is initially stimulated by nutrient secretagogues such as glucose or non-nutrient secretagogues such as acetylcholine. Glucose-stimulated insulin secretion (GSIS)[2] occurs through a well characterized pathway whereby glucose is taken up and metabolized to generate ATP, which in turn inhibits the ATP-sensitive potassium channel (K_{ATP}) resulting in depolarization of the plasma membrane and activation of the voltage-dependent Ca^{2+} channel (VDCC). In addition to VDCC-mediated Ca^{2+} influx, one or more of the transient receptor potential (TRP) channels may contribute to the rapid rise in Ca^{2+} (3). The endoplasmic reticulum (ER) has a large Ca^{2+} storage capacity and acts to both buffer the cytoplasm Ca^{2+} and to release Ca^{2+} in response to non-nutrient secretagogues. Sarcoplasmic endoplasmic reticulum Ca^{2+}-ATPase (SERCA) plays an important role in regulating ER Ca^{2+} by pumping Ca^{2+} into the ER and is required to maintain high ER Ca^{2+} levels. In the case of glucose-stimulated insulin secretion the ER acts as an important buffer for the massive influx of Ca^{2+} into the cytoplasm (4) and can extend stimulated secretion by releasing Ca^{2+} into the cytoplasm by a Ca^{2+}-induced Ca^{2+} release mechanism. Depletion of ER Ca^{2+} induces the store-operated Ca^{2+} channel (SOCC) at the plasma membrane, which not only results in ER Ca^{2+} refilling but also increases cytoplasmic Ca^{2+} stimulating insulin secretion. Although the role of ER Ca^{2+} stores in regulating insulin secretion is still incompletely understood, its importance is underscored by the observation that dysfunctions in or inhibition of SERCA residing in the ER membrane result in ablation of stimulated insulin secretion (5–8).

Besides glucose, non-fuel secretagogues such as acetylcholine or carbachol can also drive insulin exocytosis (9). Acetylcholine, released by intrapancreatic nerve endings during the preabsorptive and absorptive phases of feeding, causes the release of internal Ca^{2+} stores largely located in the ER by activating phospholipase C. Activation of phospholipase C results in the generation of inositol triphosphate (IP_3), which causes the release of ER Ca^{2+} into the cytosol via the IP_3 receptor channels (9, 10). ER Ca^{2+} release further triggers store-operated Ca^{2+} entry (SOCE) to maintain a sustained elevation of cytosolic Ca^{2+} level and insulin secretion (10, 11).

PERK (EIF2AK3), an eIF2α kinase in the ER membrane, is essential for normal development and function of the insulin-secreting β-cell (12–15). *Perk* loss of function mutations in humans and mice result in insulin-dependent permanent neo-

* This work was supported, in whole or in part, by National Institutes of Health Grant DK088140 (to D. R. C.).
[1] To whom correspondence should be addressed: 101 LSB, University Park, PA 16802. Tel.: 814-865-9790; Fax: 814-865-6193; E-mail: drc9@psu.edu.
[2] The abbreviations used are: GSIS, glucose-stimulated insulin secretion; VDCC, voltage-dependent Ca^{2+} channel; TRP, transient receptor potential; SERCA, sarcoplasmic endoplasmic reticulum Ca^{2+}-ATPase; ER, endoplasmic reticulum; SOCC, store-operated Ca^{2+} channel; IP_3, inositol triphosphate; SOCE, store-operated Ca^{2+} entry; CN, calcineurin; CPA, cyclopiazonic acid; 2-APB, 2-aminoethoxydiphenyl borate; CPM, cypermethrin; GCA, chlorogenic acid; PERK, protein kinase R (PKR)-like endoplasmic reticulum kinase; PI, phosphatidylinositol; KRB, Krebs-Ringer bicarbonate.

natal diabetes due to insufficient insulin secretion from the pancreas (12, 14). PERK has also been shown to play a key role in regulating the ER stress and the unfolded protein response in cultured cells that are subjected to severe stress conditions (16, 17). However, the relevance of the ER stress response pathway to the normal developmental and physiological functions of PERK in β-cells has been questioned and remains controversial (18, 19). Previous attempts to identify the primary functions of PERK were confounded by the myriad dysfunctions within β-cells including ablated insulin synthesis and secretion, delayed development and proliferation of the β-cells, and a massive accumulation of proinsulin in the ER (14, 19, 20) as well as dysfunctions in other organs and tissues (13, 14, 21). Recently a highly selective PERK inhibitor (denoted throughout as PERKi in text and *PI* in figure legends) was developed by GlaxoSmithKline, Inc. (22). When applied to animal models, it recapitulated the major pancreatic defects seen in *Perk*-deficient mice and humans including β-cell dysfunction and atrophy of the exocrine pancreas (22, 23). The GlaxoSmithKline (GSK) PERK inhibitor provided us the means to acutely inhibit PERK activity and assess the immediate impact on insulin secretion and intracellular Ca^{2+} dynamics in the pancreatic β-cells prior to the onset of severe cellular dysmorphies.

Calcineurin (CN) (14), a Ca^{2+}-dependent phosphatase, plays similar roles to PERK in regulating insulin secretion, β-cell proliferation, and glucose homeostasis (24, 25) suggesting that PERK and CN may be acting through related pathways. Supporting this hypothesis, Bollo and co-workers (26) discovered that CN and PERK interact and modulate each others activity as a function of the concentration of cytoplasmic Ca^{2+}. Moreover, CN has been shown to dephosphorylate calnexin and thereby relieve repression of SERCA activity and ER Ca^{2+} uptake.

We show herein that acute inhibition of PERK or CN in β-cells rapidly suppresses glucose-stimulated insulin secretion. Unexpectedly we discovered that ablation of their activities also strongly abrogates glucose-stimulated Ca^{2+} uptake into the cytoplasm and restoration of Ca^{2+} to the ER following stimulated release. We speculate that the major function of PERK in the pancreatic β-cell is to coordinate Ca^{2+} dynamics between the ER and the cytoplasm during stimulus-coupled secretion of insulin, and that this regulation is mediated through CN.

EXPERIMENTAL PROCEDURES

Reagents—GSK2606414 PERK inhibitor was a kind gift from Jeffrey Axten and Rakish Kumar, GlaxoSmithKline, Collegeville, PA. PERKi was prepared as a 10 mM stock solution in dimethyl sulfoxide and diluted immediately before use. Chlorogenic acid (Sigma), cypermethrin (Sigma), and ionomycin (Calbiochem) were dissolved in a ×10,000 dimethyl sulfoxide working concentration and diluted immediately before use.

Cell Culture—INS1 832/13 (obtained from Dr. Christopher Newgard, Duke University) and MIN6 cells (provided by Dr. Jun-Ichi Miyazaki, Osaka University, Japan) were cultured as previously described (27). *INS1* 832/13 cells containing a short-hairpin RNA directed against the rat *Perk* mRNA (*shPerk*) were obtained from Dr. Fumihiko Urano (University of Massachusetts). The *shPerk* is stably integrated into the genome of *INS1* 832/13 β-cell lines and under the inducible regulation of doxycycline. The *INS1* 832/13 *shPerk* cells were cultured in a tetracycline-free environment to avoid leaky expression of *shPerk*. Full details of treatment to various cell lines were described in figure legends.

Islet Isolation and Primary β-Cell Culture—Human pancreatic islets were obtained through the Integrated Islet Distribution Program and first allowed overnight recovery in fresh RPMI1640 medium with 10% fetal bovine serum, 1% antibiotic antimycotic solution (Sigma), and 5.5 mM glucose at 5% CO_2, 95% air. Rat islets were isolated from 2–3-month-old Sprague-Dawley rats (purchased from Charles River) using a modified Histopaque-1077 separation method (28) and cultured in the same way as human islets.

For primary β cell culture, islets were disassociated by trypsin (0.125% in PBS; 4 min at 37 °C) to release single cells and evenly plated on coverslips for 48 h before experiments. For Ca^{2+} imaging experiments utilizing cells isolated from islets we did not specifically identify β cells, which comprise ~75% of the islet. However, for all cytosolic Ca^{2+} measurements we selected cells that exhibited a positive response to glucose, which selected against α-glucagon cells that comprise ~20% of the islet and do not respond positively to high glucose stimulation (29).

Insulin Secretion—Insulin concentrations were determined by immunoassay (Meso Scale Discovery) and were normalized to total protein concentration. For studies of insulin secretion, isolated islets or cultured β-cell line were first cultured overnight at 37 °C (5% CO_2) in RPMI1640 medium containing 10% fetal bovine serum and 5.5 mM glucose. Samples were then incubated at 37 °C in KRB-HEPES buffer (pH 7.4) with 1% bovine serum albumin for assigned pretreatment and insulin stimulation as described in figure legends. At the end of the 30-min stimulation, the supernatant was assayed for secreted insulin (by Meso Scale Discovery), and cells/islets were sonicated in acid ethanol and assayed for total insulin (by Meso Scale Discovery) and total protein (by Bio-Rad Protein Assay).

Immunocytochemistry—Cultured β-cells were subjected to fixation and permeabilization with 4% formaldehyde and 0.1% Triton X-100. The cells were then denatured with 1 N HCl for 20 min, followed by 5% horse serum (Invitrogen) in PBS for 1 h. The following primary antibodies were applied overnight at 4 °C: insulin (1:500, Abcam), proinsulin (1:200, Beta Cell Biology Consortium and Hytest), and NFATc1 (1:200, Thermo Scientific). Appropriate secondary antibodies conjugated with Alexa Fluor 350, 488, or 555 dye (Molecular Probes) were used (1:400 dilution) to visualize the labeled cells. Anti-fade reagent with DAPI (Invitrogen) was used to mount slides and label nucleic region. Fluorescence images were captured with a Nikon Eclipse E1000 and Image-Pro Plus (Phase 3 Imaging Systems, GE Healthcare, Inc.).

For NFATc1 translocation measurement, all procedures for immunocytochemistry and image collection were done at the same time under identical conditions to allow direct comparison between treatments. For data analysis, NIH Image J software was used. The nucleic and cytosolic areas were traced based on DAPI and the insulin signal, and after background subtraction for each area, NFATc1 translocation was quanti-

fied for each cell by calculating ratio of pixel density of NFATc1 in the nucleic area to the density in cytoplasm.

Voltage-dependent Ca^{2+} Current Density Measured by Whole Cell Patch Clamp—Whole cell patch clamp recordings were performed using the Multiclamp 700A patch clamp amplifier (Molecular Devices, Palo Alto, CA). Tetrodotoxin (1 μM) and tetraethylammonium (15 mM) were added during recording to block voltage-dependent sodium channels and potassium channels. For Ca^{2+} current recording experiments, the membrane potential was held at −70 mV baseline. A series of depolarizing voltage steps with 10-mV increments were delivered at 5-s intervals, to elicit voltage-dependent Ca^{2+} responses. Data were collected using pClamp 9 software (Molecular Devices, Palo Alto, CA), sampled at 10 kHz and filtered at 1 kHz. Off-line data analyses of Ca^{2+} currents amplitude were performed using pClamp 9 software. All experiments were performed at room temperature.

Immunoprecipitation and Western Blots—Immunoprecipitation was performed using the Protein G Immunoprecipitation Kit (Sigma). 5 μl of SERCA N1 antiserum (gift from Dr. Jonathan Lytton, University of Calgary, Canada) was used for each sample. For protein assay from whole cells, total *INS1* 832/13 cellular proteins were extracted with RIPA buffer (1% Nonidet P-40, 0.5% sodium doxycholate, 0.1% SDS, 1× PBS, pH 8.0) containing 1× protease and phosphatase inhibitor mixtures (Sigma). IP or whole cellular protein samples were boiled in 2× SDS sample buffer and then loaded onto 4–15% gels for Western blots. Primary antibodies used in the analysis were: anti-eIF2α-P (1:500, Invitrogen), anti-tubulin (1:1000, Sigma), anti-PERK (1:500, Cell Signaling), anti-pPERK (1:500, Cell Signaling), anti-SERCA N1 (1:5000), and anti-calnexin (1:1000, Enzo Life Sciences).

PERK autophosphorylation was measured using anti-PERK blot. Phosphorylated PERK band (PERK(P)) and total PERK band (PERK) of each sample were traced and the pixel density was measured for each sample with background subtraction.

Cytosolic Ca^{2+} Measurement by Fura2 Ca^{2+} Imaging—The cytosolic Ca^{2+} level was measured using the ratiometric Ca^{2+} indicator Fura2-AM following the procedure of Roe and co-workers (30). After dye loading, coverslips (12 mm) were transferred to a perfusion chamber (Warner Instruments Series 20 open bath chamber) mounted on a Nikon TE-2000-S inverted microscope with a ×20 objective and a high 340/380 nm transmittance filter for Ca^{2+} ratio imaging (Chroma Technology). Cells were perfused in KRB-HEPES with a constant flow rate of 1–2 ml/min at 37 °C. Details of treatment were described in figure legends. Multiple cells were randomly picked per operation. Ratios of the fluorescent emission signals under excitation at 340 over 380 nm (R) were collected by Simple PCI imaging software (C-Imaging) and further normalized to the average ratios before stimulation (R_0).

ER Ca^{2+} Measurement by Fluorescence Resonance Energy Transfer (FRET)-based Ca^{2+} Imaging with ER-targeted Cameleon—ER Ca^{2+} level was measured using FRET-based D1ER cameleon probe following the protocol of Michael Roe and co-workers (30). Cells were transduced with adenovirus encoding the ER-targeted cameleon D1ER (provided by Dr. Michael Roe, SUNY Upstate Medical University). The medium was replaced with fresh RPMI1640 medium after 2 h of transduction and cultured for an additional 48 h before experiments. Coverslips (25 mm) were placed into a glass coverslip dish (mode MSC-TD, Warner instruments) fit on PDMI-2 microincubator (Harvard Apparatus). Cells were perfused with KRB-HEPES buffer at a constant rate of 3 ml/min at 37 °C. Full details of treatments were provided in the figure legends. Images were obtained at 5-s intervals using a Nikon Eclipse E600FN microscope with a ×60 1.0 numerical aperture water immersion objective (Nikon) controlled by Metavue software (Universal Imaging Corp.). Filters used for the dual emission ratio (CFP excitation 430/25, CFP emission 470/30; YFP emission 560/80) were placed in filter wheels and combined with the dual dichroic mirror at 505 nm (505dcxr, Chroma). Data were represented as ratios of YFP over CFP signal intensity (R) normalized to the average ratios prior to stimulation (R_0). The samples used for the ER Ca^{2+} experiments on primary human and rat islet cells were from the same batch of islets as those used the for cytosolic Ca^{2+} experiments. The β-cell fraction was estimated based on cytosolic Ca^{2+} measurement under glucose stimulation.

Statistical Analysis—All numeric data were represented as mean ± S.E. For Ca^{2+} imaging data, results are presented as averages from >3 separate experiments. The area under the curve was measured for each biological individual and used to estimate the percentage difference between treatments. Statistical significance was determined using Student's t testing.

RESULTS

Inhibition of PERK Activity Recapitulates β-Cell Dysfunctions Seen in Genetic Ablation of Perk—Previously we showed that loss of function mutations of *Perk* in mice (*PKO*) led to an impacted ER phenotype in a substantial fraction of β-cells (30–40%) characterized by accumulation of proinsulin and other client proteins in the ER and failure of anterograde trafficking to the Golgi (19, 20, 27). This phenotype can be readily detected using immunohistochemical labeling of insulin and proinsulin in mouse islets of Langerhans (Fig. 1*A*, *top*). To test whether inhibition of the enzymatic activity of PERK results in the impacted-ER phenotype, we employed the use of newly developed PERK inhibitor GSK2606414, which is a high affinity ligand of the catalytic site that competes with ATP (22, 23). Approximately 20% of the *INS1* 832/13 cells treated 24 h with 1 μM PERKi exhibited the same impacted ER phenotype seen in *PKO* mice (Fig. 1*A*, *lower view*). We next determined whether PERKi reduced PERK activity. Depletion of ER Ca^{2+} stores causes activation of PERK and phosphorylation of its substrate eIF2α (31, 32). Exposing *INS1* 832/13 cells 30 min to cyclopiazonic acid (CPA), an inhibitor of SERCA, led to PERK activation and phosphorylation of eIF2α (Fig. 1*B*, *lanes 4*, *8*, and *12*). Pre-treatment with PERKi for 20 min abolished CPA-induced PERK activation and eIF2α phosphorylation (Fig. 1*B*, *lanes 3*, *7*, and *11*). Therefore the PERKi can be used as an effective tool for investigating the immediate effects of PERK inhibition on the scale of minutes, which is ~20 h before severe cellular dysfunctions are first seen.

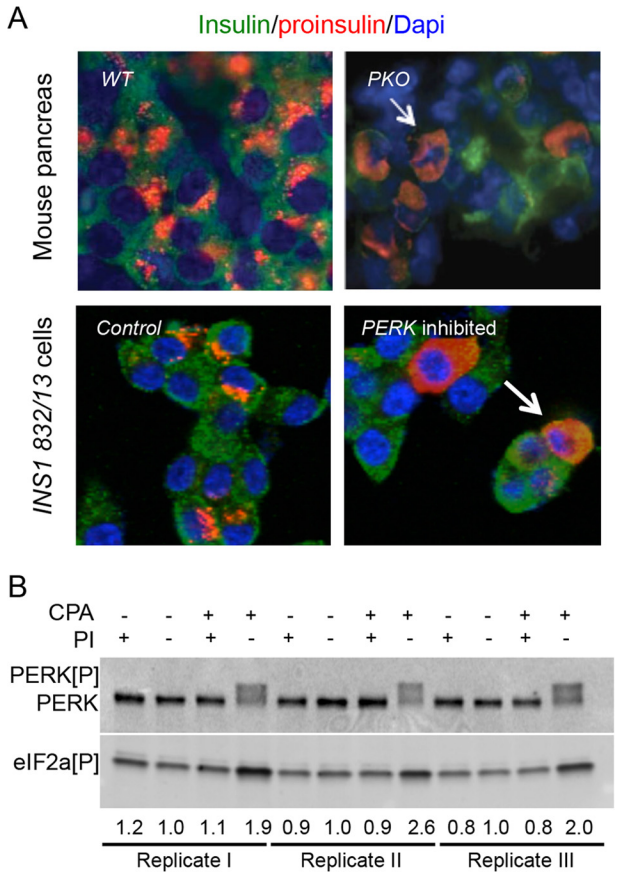

FIGURE 1. **Inhibition of PERK activity recapitulates β-cell dysfunctions found in the Perk genetic ablation model.** *A,* immunostaining of β-cells using insulin, proinsulin, and DAPI. *Top view* illustrates the pancreatic section from WT and *PKO* P1 mice. *Bottom view* shows staining of *INS1* 832/13 cells pre-treated by the GSK414 PERK inhibitor (*PI*) or vehicle for 24 h. *B,* representative Western blot showing phosphorylation levels of PERK and eIF2α in *INS1* cells. Samples were treated with 1 μM PI or vehicle for 20 min followed by co-treatment with or without CPA for another 30 min before protein extraction. Quantification of phosphorylated eIF2α is expressed as fold change relative to non-CPA and non-PI controls.

Acute Inhibition of PERK Activity Impairs Glucose-dependent Insulin Secretion—Previously we showed that glucose-stimulated insulin secretion was ablated in islets isolated from neonatal *PKO* mice (19). In the present study, this result was confirmed by genetic knockdown of *Perk* in *INS1* 832/13 β-cells bearing a tetracycline-operated *shPerk* transgene (denoted as *INS1* 832/13 *shPerk* cells). After 24 h administration of 2 μg/ml of doxycycline, the *Perk* mRNA level was reduced to 39.7 ± 3.9% of WT cells ($n = 6$, $p < 0.001$) and GSIS was reduced by 57.6 ± 2.2% ($p < 0.001$, Fig. 2*A*). To determine whether acute inhibition of PERK by PERKi impacts insulin secretion, PERKi was employed for 20 min before 20 mM glucose stimulation. PERK inhibition led to reduction of GSIS in *INS1* 832/13 cells (Fig. 2*B*, *left panel*) and in islets isolated from rats (Fig. 2*B*, *middle panel*) and humans (Fig. 2*B*, *right panel*) by 34.6 ± 3.8% ($p < 0.01$), 27.1 ± 9.0% ($p = 0.058$), and 35.6 ± 5.4% ($p < 0.01$), respectively. In addition, we also measured insulin secretion of INS1 832/13 cells in response to 8 mM glucose, which is a more physiological concentration observed postprandially. PERK inhibition also led to a reduction of GSIS by 22.0 ± 3.6% ($p < 0.001$, Fig. 2*C*). Because an increase in $[Ca^{2+}]_c$ is a key regulator of GSIS, we measured the effect of PERKi on glucose-stimulated changes in $[Ca^{2+}]_c$ in rat and human pancreatic islets of Langerhans. Pretreatment with 1 μM PERKi for 20 min significantly lowered the glucose-induced rise in $[Ca^{2+}]_c$ by 61.9 ± 13.3% ($p < 0.01$) in rat islets and 55.9 ± 8.4% ($p = 0.053$) in human islets (Fig. 2*D*). These results indicate that PERK activity is required for normal glucose-stimulated insulin secretion and suggests this modulation is mediated by mechanisms underlying Ca^{2+} signaling.

PERK Inhibition Represses Stimulated Ca^{2+} Influx—Glucose-stimulated Ca^{2+} signaling is regulated by Ca^{2+} influx through the plasma membrane and release of Ca^{2+} from ER Ca^{2+} stores (33, 34). *INS1* 832/13 cells perfused with 25 mM KCl exhibited a rapid increase in $[Ca^{2+}]_c$ that required extracellular Ca^{2+}. In Ca^{2+}-free solutions, the $[Ca^{2+}]_c$ increase in response to high K^+ was completely ablated ($p < 0.001$, Fig. 3*A*), indicating that the extracellular pool of Ca^{2+} is the primary source of Ca^{2+} under KCl stimulation. We used *Perk* shRNA and PERKi to determine whether PERK affected $[Ca^{2+}]_c$ influx induced by KCl. The uptake of Ca^{2+} was reduced by 42.6 ± 3.1% in response to KCl stimulation ($p < 0.001$, Fig. 3*A*) in *INS1* 832/13 24 h after activation of *Perk* shRNA. Treatment of *INS1* 832/13 cells with PERKi for 20 min before KCl stimulation led to a 39.4 ± 3.1% reduction in Ca^{2+} influx ($p < 0.001$, Fig. 3*A*) and a 30.8 ± 5.0% reduction in insulin secretion ($p < 0.01$, Fig. 3*B*). In addition, PERKi (1 μM, 20 min) reduced KCl-stimulated $[Ca^{2+}]_c$ by 44.1 ± 3.1% in rat ($p < 0.001$) and 40.9 ± 9.3% in human ($p < 0.05$) primary β-cells (Fig. 3, *C* and *D*). These findings suggested that PERK-dependent Ca^{2+} influx contributes to insulin exocytosis. To determine how rapidly PERKi reduced KCl-stimulated Ca^{2+} uptake, *INS1* 832/13 cells were exposed to PERKi only 100 s prior to a series of 25 mM KCl pulses. The inhibitory effect of PERKi was first detected only 10 min ($p < 0.001$, Fig. 3*E*) after addition of the inhibitor. To determine whether PERK activity was modulated by changes in $[Ca^{2+}]_c$, the autophosphorylation level of PERK was measured in β-cells treated with 50 mM KCl. PERK autophosphorylation was induced by 50 mM KCl in the Ca^{2+}-contained solution but not in the Ca^{2+}-free solution (Fig. 4*A*), suggesting that an increase in $[Ca^{2+}]_c$ induced PERK activation. We also found a significant elevation of PERK activity by exposing cells to 50 mM $CaCl_2$ (Fig. 4*B*). Taken together, these findings suggest that PERK activity is both activated by increases in $[Ca^{2+}]_c$ and regulates Ca^{2+} influx through the plasma membrane.

PERK Inhibition Does Not Directly Affect VDCC Current—Ca^{2+} influx through VDCCs plays a dominant role in contributing to the rise in $[Ca^{2+}]_c$ after stimulation of β-cells with high glucose or KCl. To determine whether PERKi negatively regulates the VDCC, VDCC-dependent Ca^{2+} current density was measured by patch clamp electrophysiology. Unexpectedly, in cells treated with PERKi, VDCC current density was not significantly different from control cells (Fig. 5*A*) suggesting that the PERK-dependent regulation of Ca^{2+} uptake involves other Ca^{2+} or ion channels.

Store-operated Ca^{2+} Entry Is Impaired by Acute PERK Inhibition—Pancreatic β-cells express other plasma membrane Ca^{2+} channels including store-operated Ca^{2+} channels and transient receptor potential channels that either conduct Ca^{2+}

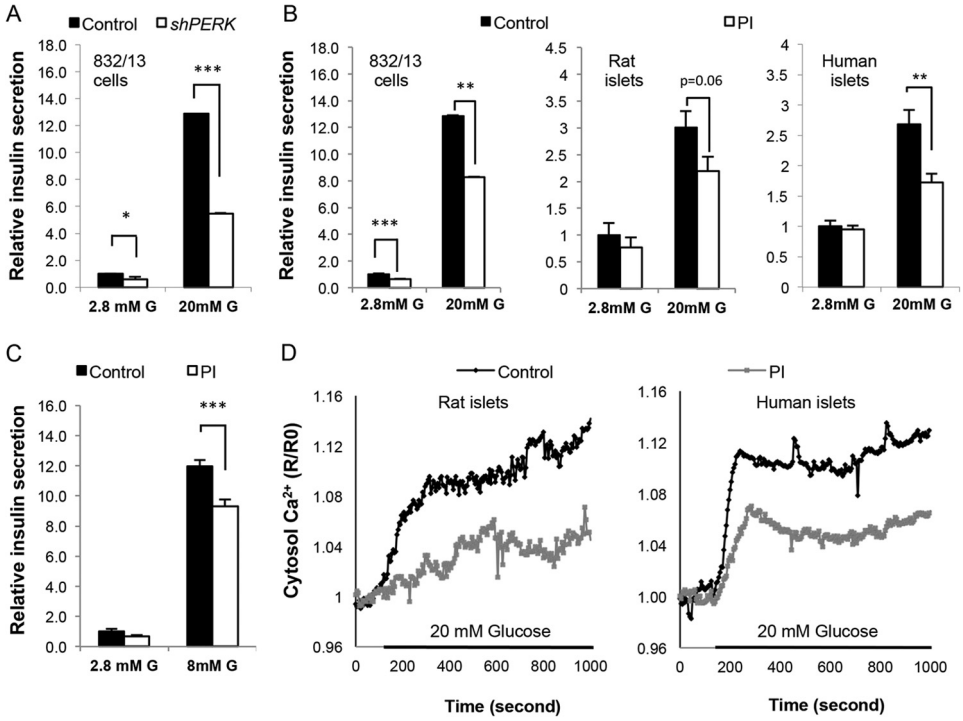

FIGURE 2. **Acute inhibition of PERK activity impairs glucose-dependent stimulus-secretion coupling.** *A,* insulin secretion in response to 2.8 or 20 mM glucose in *INS1* 832/13 *shPerk* cells pre-treated with or without doxycycline for 24 h. Cells were incubated in 2.8 mM glucose 1 h before insulin stimulation with low or high glucose. Insulin secretion was normalized to total protein and expressed as fold-increase relative to basal insulin secretion (2.8 mM glucose) of control. Shown are mean ± S.E. ($n = 4$, *, $p < 0.05$; **, $p < 0.01$; ***, $p < 0.001$). *B*, insulin secretion in response to 2.8 or 20 mM glucose in *INS1* 832/13 cells (*left panel*, $n = 14$), rat islets (*middle panel*, $n = 5$), and human islets (*right panel*, $n = 12$). Samples were incubated in 2.8 mM glucose for 1 h before experiments with vehicle or 1 μM PI added during the last 20 min. Data are analyzed and represented as described in *A* (**, $p < 0.01$; ***, $p < 0.001$). *C,* insulin secretion in response to 2.8 or 8 mM glucose in *INS1* 832/13 cells. Cells were incubated in 2.8 mM glucose for 1 h before experiments with vehicle or 1 μM PI added during the last 20 min. Data are analyzed and represented as described in *A* ($n = 6$, ***, $p < 0.001$). *D,* $[Ca^{2+}]_c$ of rat (*left panel*, $n > 12$) and human (*right panel*, $n > 3$) islets was measured by Fura2-AM and expressed as a 340 nm/380 nm ratio (*R*) relative to the basal level before stimulation (R_0) (R/R_0). Samples were treated with 2.8 mM glucose for 1 h with 1 μM PI or vehicle added in the last 20 min before Ca^{2+} administration. Shown are means of biological individuals. (Quantification by calculating area under the curve (*AUC*), rat islets: control = 100 ± 11.9%, PI = 38.1 ± 13.3%, $p < 0.05$; human islets: control = 100 ± 16.6%, PI = 44.1 ± 8.4%, $p < 0.05$).

or modulate the membrane potential (33). 2-Aminoethoxydiphenyl borate (2-APB) has been shown to inhibit SOCCs and some of the TRP channels (3, 35). We found that 2-APB and PERKi exhibit similar effects on KCl-stimulated Ca^{2+} influx, and the combination of 2-APB and PERKi showed no further reduction in Ca^{2+} influx (Fig. 5*B*). Moreover, 2-APB treatment reduced KCl-stimulated insulin secretion by 55.8 ± 2.2% in *INS1* 832/13 cells ($p < 0.001$, Fig. 5*C*). Taken together, these findings suggested that PERKi and 2-APB inhibit the same Ca^{2+} signaling mechanism, which plays a significant role in regulating insulin secretion.

To determine whether SOCC activity is affected by acute ablation of PERK, store-operated Ca^{2+} entry was measured by using 250 μM carbachol following the methods of Liu and Gylfe (11). PERK inhibition had no effect on the initial peak in cytosolic Ca^{2+} (Fig. 5, *D* and *E*), which is driven by ER Ca^{2+} release. However, the second phase, characterized by a gradual decrease and plateau, was reduced by 31.0 ± 7.0% in PERK-inhibited cells ($p < 0.05$, Fig. 5*D*). Extracellular Ca^{2+} influx through SOCC is known to be the source of the second phase (11), which was confirmed by the absence of a second phase when extracellular Ca^{2+} was absent (Fig. 5*E*). To determine whether this negative impact of PERK inhibition on SOCC may adversely impact carbachol-stimulated insulin secretion, *INS1* 832/13 cells were pretreated with PERKi and then stimulated with carbachol. PERK inhibition reduced carbachol-stimulated insulin secretion by 57.4 ± 7.1% ($p < 0.05$, Fig. 5*F*).

An alternate method to measure SOCC activity (36) was utilized to determine the effect of PERKi on SOCE. In these studies, cells were bathed in Ca^{2+}-free solutions and then ER Ca^{2+} stores were depleted using the SERCA inhibitor CPA. $[Ca^{2+}]_c$ was measured after reconstituting extracellular Ca^{2+} in the presence of a VDCC inhibitor nifedipine. The resultant Ca^{2+} influx reflected SOCE through SOCCs. As expected, administration of extracellular Ca^{2+} lead to a rapid increase of $[Ca^{2+}]_c$ that was attenuated by 21.7 ± 1.9% in *INS-1* 832/13 cells ($p < 0.05$, Fig. 5*G*) and 43.9 ± 5.0% in primary rat β-cells ($p = 0.18$, Fig. 5*H*) pretreated with PERKi.

PERK Regulates ER Ca^{2+} Reuptake through Modulation of SERCA Pump Activity—To determine whether acute loss of PERK activity impacts ER Ca^{2+} dynamics, ER Ca^{2+} levels in response to carbachol were measured using the FRET-based probe D1ER cameleon (37). Application of 250 μM carbachol in *INS1* 832/13 cells led to an immediate loss of ER Ca^{2+} followed by a rapid reuptake (Fig. 6*A*). Consistent with the absence of an effect of PERK inhibition on the transient increase in $[Ca^{2+}]_c$ following carbachol administration (Fig. 5, *D* and *E*), PERKi did not affect the rate or extent of Ca^{2+} extrusion from the ER (Fig. 6*A*). However, ER Ca^{2+} reuptake was significantly reduced by 41.5 ± 10.2% in PERK-inhibited cells ($p < 0.05$, Fig. 6*A*). More-

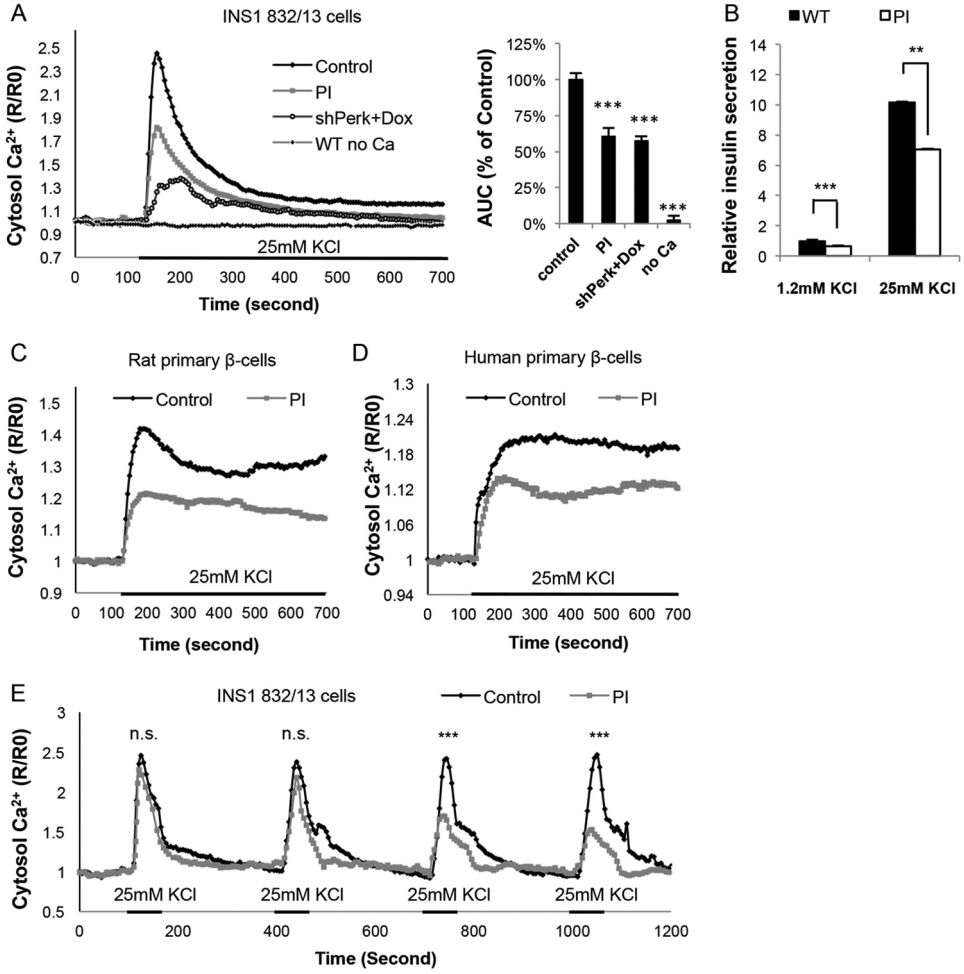

FIGURE 3. **PERK regulates Ca^{2+} influx and insulin exocytosis under high K^+ stimulation.** *A*, $[Ca^{2+}]_c$ of *INS1* 832/13 β-cells in response to 25 mM KCl with the presence of 3 mM glucose was measured by Fura2-AM and represented as R/R_0. Cells were exposed to 1 μM PERK for 20 min before Ca^{2+} administration. *INS1* 832/13 *shPerk* cells were treated with or without doxycycline (2 μg/ml) for 24 h before experiments. Ca^{2+} traces (*left*) shown as means of biological individuals and quantifications (*right*) were done by calculating the area under the curve (*AUC*) ($n > 50$). *B,* insulin secretion in response to 1.2 or 25 mM KCl with the presence of 3 mM glucose in *INS1* 832/13 cells pre-treated with vehicle or 1 μM PI for 20 min. Data are analyzed and represented as described in *A* ($n > 4$, **, $p < 0.01$; ***, $p < 0.001$). *C,* $[Ca^{2+}]_c$ of rat primary β-cells in response to 25 mM KCl with the presence of 3 mM glucose measured by Fura2-AM. Experiments were performed and analyzed the same as *A* ($n > 26$, AUC: control = 100 ± 9.1%, PI = 55.9 ± 5.5%, $p < 0.001$). *D,* $[Ca^{2+}]_c$ of human primary β-cells in response to 25 mM KCl with the presence of 3 mM glucose measured by Fura2-AM. Experiments were performed and analyzed the same as *A* ($n > 18$, AUC: control = 100 ± 13.3%, PI = 59.1 ± 9.3%, $p < 0.05$). *E,* $[Ca^{2+}]_c$ of *INS1* 832/13 cells in response to 25 mM KCl with the presence of 3 mM glucose. Vehicle or 1 μM PI were added at 0 s of $[Ca^{2+}]_c$ administration ($n > 20$, significance was determined by comparing peak values, ***, $p < 0.001$). *n.s.*, not significant.

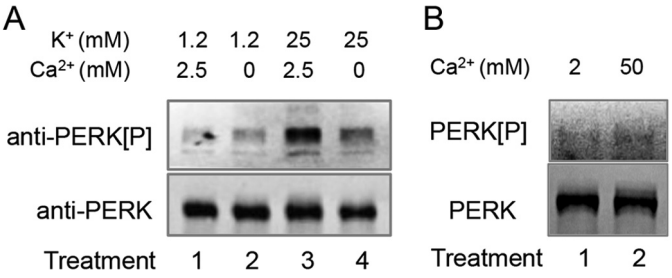

FIGURE 4. **PERK activity is modified by changes of cytosolic Ca^{2+}.** *A,* representative Western blots showing PERK autophosphorylation in response to 25 mM KCl in the presence or absence of 2.5 mM extracellular Ca^{2+}. MIN6 mouse β-cells were incubated in KRB buffer with the indicated K^+ and Ca^{2+} concentrations for 30 min and harvested for immunoblot. Pixel density of the phosphorylated PERK blot to the total PERK blot was calculated for each sample ($n = 5$, treatment 1 *versus* 3: $p < 0.05$; 3 *versus* 4: $p < 0.05$). *B,* representative Western blots showing PERK autophosphorylation in response to 2 or 50 mM $CaCl_2$. MIN6 mouse β-cells were preincubated in KRB buffer with 2 mM Ca^{2+} for 1 h and switched to the indicated Ca^{2+} concentrations for 30 min and subjected to analysis and quantification as described in *A* ($n = 4$, treatment 1 *versus* 2: $p < 0.05$).

over, this effect of PERKi was not mediated through 2-APB-sensitive channels (Fig. 6*B*), suggesting that PERK may regulate SERCA-mediated ER Ca^{2+} reuptake independently of its effects on SOCE. To explore this possibility, we estimated SERCA pump activity using an alternative method (31), which utilizes the reversible SERCA inhibitor CPA. Control cells treated with vehicle showed rapid refilling of ER after wash-out of CPA, whereas in PERK-inhibited ER Ca^{2+} restoration was reduced by 76.1 ± 5.2% ($p < 0.01$, Fig. 6*C*, *left panel*). PERKi also attenuated the ER Ca^{2+} refilling by 56.2 ± 6.8% in primary rat β-cells ($p < 0.05$, Fig. 6*C*, *middle panel*) and 39.6 ± 6.7% in primary human β-cells ($p < 0.01$, Fig. 6*C*, *right panel*). Taken together, our data suggest that PERK positively regulates SERCA particularly when ER Ca^{2+} stores are being replenished.

Interaction of SERCA and Calnexin Is Negatively Regulated by PERK—SERCA pump activity is negatively regulated through interaction with calnexin, an ER chaperone protein

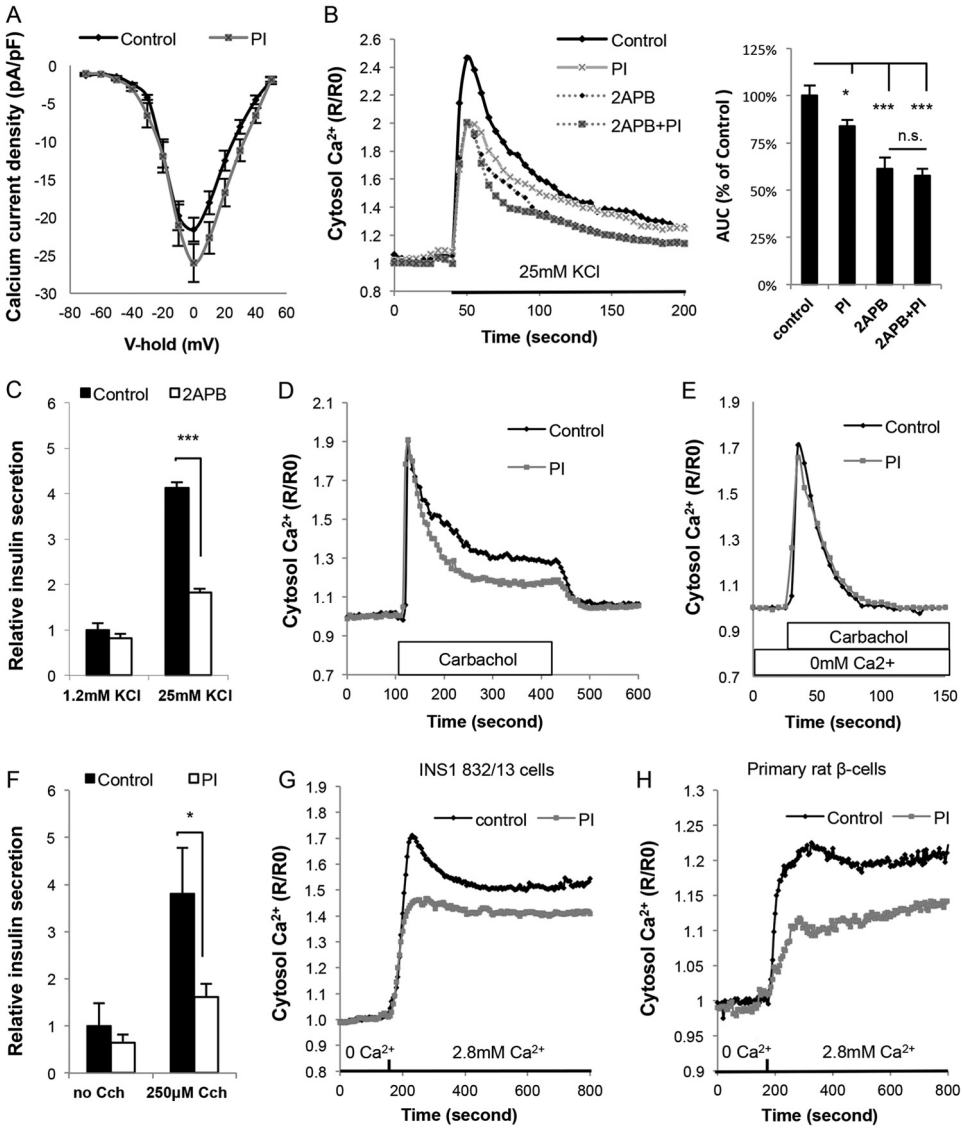

FIGURE 5. **Store-operated Ca^{2+} entry is impaired by acute PERK inhibition, whereas VDCC activity is not affected.** *A,* VDCC current density of *INS1* 832/13 cells was measured by patch clamp after 20 min treatment of vehicle or 1 μM PI. Shown are mean ± S.E. ($n = 22$, neither peak value nor AUC showed significant differences between treatments). *B,* $[Ca^{2+}]_c$ of *INS1* 832/13 cells in response to 25 mM KCl. Cells were exposed to the indicated chemical 20 min before experiments. Ca^{2+} traces are shown as means of biological individuals. *Bar graph* shows quantifications by calculating AUC (% of control) ($n > 17$, *, $p < 0.05$; ***, $p < 0.001$). *C,* insulin secretion of *INS1* 832/13 cells in response to 1.2 or 25 mM KCl in the presence of 3 mM glucose. Cells were treated with vehicle or 2-APB (100 μM) for 20 min before the experiment. Data are analyzed and represented as described in Fig. 2*A* ($n = 6$, ***, $p < 0.001$). *D,* $[Ca^{2+}]_c$ in response to carbachol was measured by Fura2-AM in hyperpolarized *INS1* 832/13 cells after 1 h exposure to 400 μM diazoxide plus 20 mM glucose and 2.8 mM Ca^{2+}, with vehicle or 1 μM PI added in the last 20 min. Shown are means of biological individuals ($n > 9$, area under the curve (*AUC*): control = 100 ± 11.1%, PI = 69.0 ± 7.0%, $p < 0.05$). *E,* $[Ca^{2+}]_c$ of *INS1* 832/13 cells in response to carbachol in Ca^{2+}-free medium was measured using Fura2-AM. Cells were exposed to PI or vehicle 20 min before the experiment. Shown are means of biological individuals ($n > 21$, AUC: control = 100 ± 9.5%, PI = 109.0 ± 9.8%, *n.s.*, not significant). *F,* insulin secretion of *INS1* 832/13 cells in response to carbachol. Cells were pretreated with 400 μM diazoxide plus 20 mM glucose and 2.8 mM Ca^{2+} for 1 h, with vehicle or PI added in the last 20 min. Shown are mean ± S.E. ($n = 4$, *, $p < 0.05$). *G,* SOCC-mediated Ca^{2+} influx in *INS1* 832/13 cells measured by Fura2-AM. Vehicle or PI were added in 2.8 mM KRB buffer for 10 min. Samples were then perfused with 10 μM CPA, 100 μM nifedipine, 100 μM EGTA in Ca^{2+}-free KRB for 10 min before Ca^{2+} measurement. Shown are means of biological individuals ($n = 44$, AUC, control = 100 ± 9.0%, PI = 78.3 ± 1.9%, $p < 0.01$). *H,* SOCC-mediated Ca^{2+} influx in primary rat β-cells was measured following the same procedure and analysis as described in *G* ($n = 14$, AUC: control = 100 ± 39.4%, PI = 56.1 ± 5.0%, $p = 0.18$).

(26, 38). To determine whether PERK affects the interaction between SERCA and calnexin, a co-immunoprecipitation experiment with SERCA antibody was performed. Cells treated with PERKi showed a 2.4-fold increase in calnexin coimmunoprecipitated with SERCA (Fig. 6, *D* and *E*), suggesting that PERK negatively regulates the interaction of SERCA and calnexin in β-cells. This result is consistent with our finding that PERK positively regulates SERCA pump activity.

Calcineurin Is a Downstream Mediator of PERK Signaling in β-Cells—Previous studies in other mammalian and amphibian cell types showed that calcineurin, a Ca^{2+}-dependent protein phosphatase (14), interacts with PERK, and dephosphorylates calnexin (26). This raises the possibility that PERK regulates SERCA activity and SOCE in β-cells through a CN-dependent pathway. First, we determined whether inhibition of PERK affected CN activity as measured by NFATc1 translocation (39)

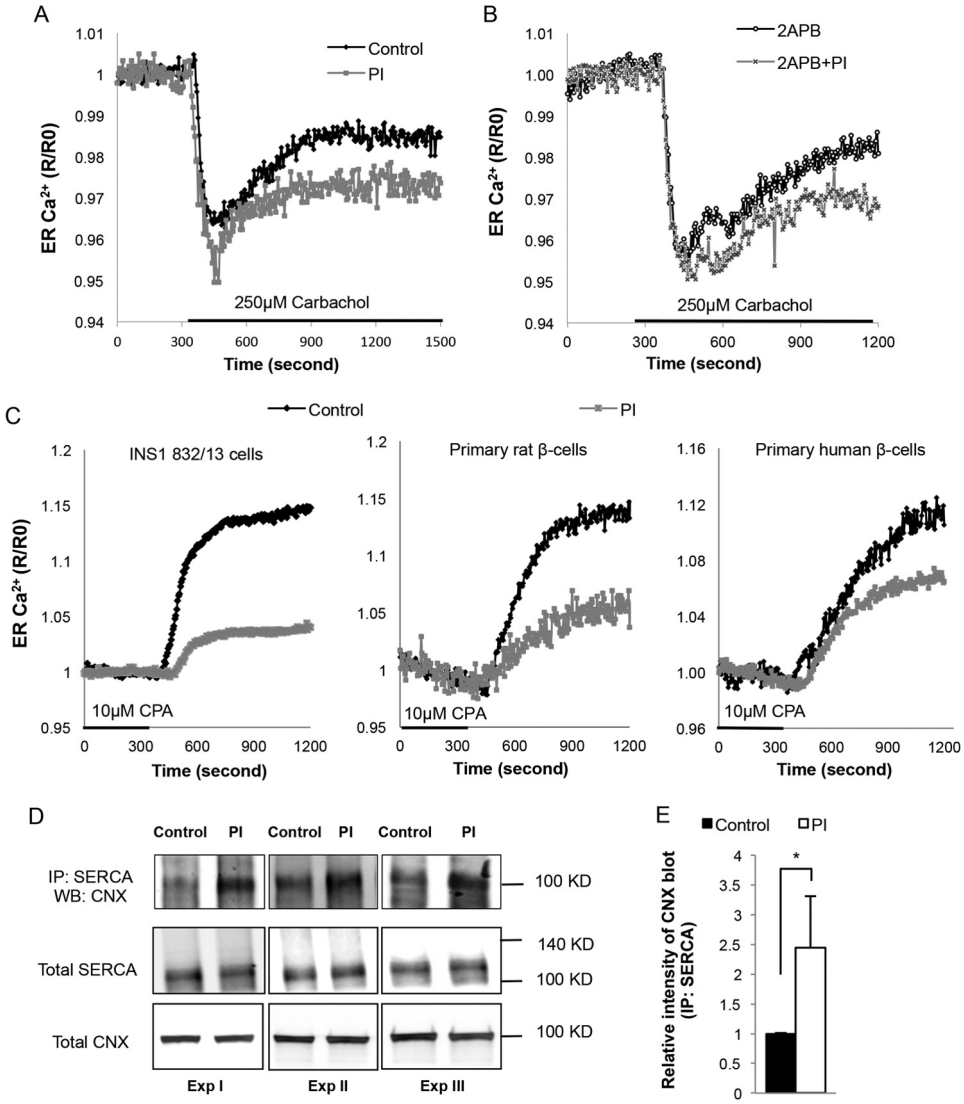

FIGURE 6. **PERK regulates ER Ca^{2+} reuptake through modulation of SERCA pump activity.** *A,* $[Ca^{2+}]_{ER}$ of *INS1* 832/13 cells in response to carbachol was measured using FRET-based probe D1ER cameleon and expressed as a YFP/CFP ratio (*R*) normalized to that before stimulation (R_0) (R/R_0). Cells were exposed to PI or vehicle 20 min before the experiment. Shown are means of biological individuals ($n > 5$, area under the curve (*AUC*) of ER Ca^{2+} uptake phase: control = 100 ± 7.4%, PI = 58.5 ± 10.2%, $p < 0.05$). *B,* $[Ca^{2+}]_{ER}$ of *INS1* 832/13 cells in response to carbachol was measured by FRET-based D1ER probe. Cells were exposed to 2-APB with or without PI for 20 min before experiment. Data are represented as means of all biological individuals ($n > 5$, AUC of ER Ca^{2+} uptake phase: control = 100 ± 11.9%, PI = 60.2 ± 18.4%, $p = 0.051$). *C,* SERCA-mediated ER Ca^{2+} reuptake of *INS1* 832/13 cells (*left*, $n > 5$), primary rat islet cells (*middle*, $n > 4$), and primary human islet cells (*right*, $n > 5$). Based on estimation of the β-cell fraction from glucose-stimulated cytosolic Ca^{2+} measurement, 75% of the cells measured were β-cells. Samples were pre-treated with 20 mM glucose in KRB for 1 h with CPA plus vehicle/PI added in the last 20 min. Shown are means of biological individuals (quantification of AUC showed: *left*, control = 100 ± 12.3%, PI = 23.9 ± 5.2%, $p < 0.01$; *middle*, control = 100 ± 16.4%, PI = 43.8 ± 6.8%, $p < 0.05$; *right*, control = 100 ± 11.9%, PI = 60.4 ± 6.7%, $p < 0.01$). *D,* representative Western blots (*WB*) from three independent experiments showing calnexin (*CNX*) protein immunoprecipitated (*IP*) with SERCA antibody. *INS1* 832/13 cells were pretreated with 20 mM glucose in KRB for 1 h, with CPA plus PI/vehicle added in the last 20 min. *E,* quantitative analysis of IP Western by measuring pixel density of blots. Data represent as intensity of CNX blot relative to WT control and shown as mean ± S.E. ($n = 12$, *, $p < 0.05$).

(40). Cells exposed to PERKi and cypermethrin (CPM), an inhibitor of CN (41), exhibited decreased levels of NFATc1 translocation ($p < 0.05$, Fig. 7*A*), suggesting that PERK positively regulates CN activity. In contrast, chlorogenic acid (CGA), an activator of CN (42), resulted in a 60.4 ± 19.9% increase of NFATc1 translocation ($p < 0.05$, Fig. 7*A*). Moreover, CGA relieved the block of NFATc1 translocation imposed by PERKi ($p < 0.001$, Fig. 7*A*).

These findings raised the possibility that the interplay between PERK and CN is an important regulatory component of subcellular Ca^{2+} signaling dynamics in pancreatic β-cells. To directly test whether CN regulates Ca^{2+} dynamics, *INS1* 832/13 cells were treated with the CN inhibitor CPM. CN-inhibited cells showed a 59.7 ± 5.7% reduction in cytosolic Ca^{2+} influx ($p < 0.001$, Fig. 7*B*) and a 65.9 ± 4.7% reduction in insulin secretion ($p < 0.01$, Fig. 7*C*) in response to 25 mM KCl, which was similar to the impact of PERK inhibition. We further determined whether SOCE was affected by CN activity. Cells treated with CPM exhibited a 38.0 ± 4.7% ($p < 0.001$) decrease in SOCE (Fig. 7, *D* and *E*), whereas activation of CN by CGA restored SOCE in the PERK-inhibited cells to control levels ($p < 0.05$, Fig. 7, *D* and *E*). As expected, SOCE in CPM-treated samples could not be recovered by CN activator CGA (Fig. 7*F*). Furthermore, cells treated with CPM showed a 78.0 ± 3.9%

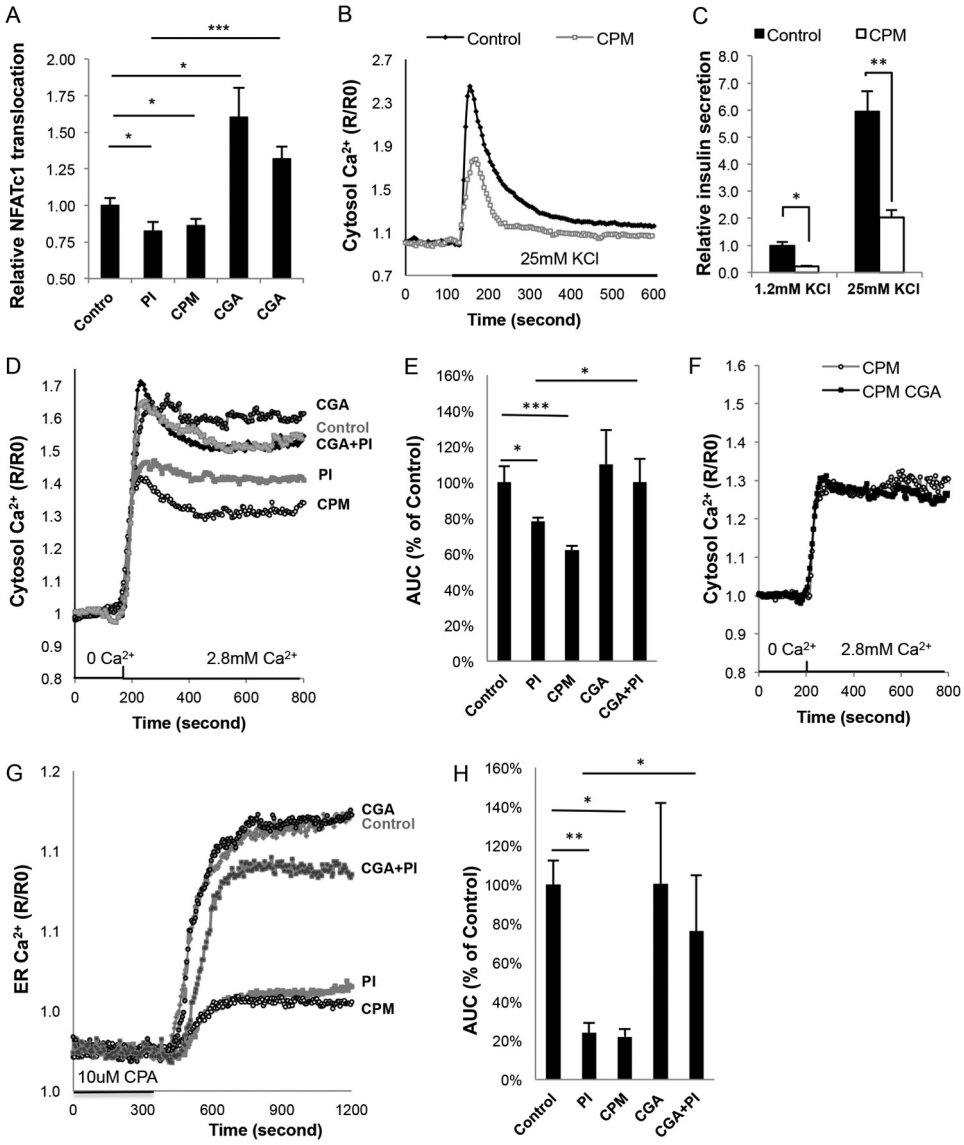

FIGURE 7. **Calcineurin is a downstream mediator of PERK signaling in β-cells.** *A,* NFATc1 translocation in *INS1* 832/13 cells measured by immunocytochemistry and data are represented as fold-changes relative to WT control. Cells were treated with the indicated chemical for 20 min followed by co-treatment with ionomycin for an addition 1 h before immunocytochemistry. Shown are mean ± S.E. ($n = 5$, *, $p < 0.05$; ***, $p < 0.001$). *B,* $[Ca^{2+}]_c$ of *INS1* 832/13 cells in response to 25 mM KCl measured by Fura2-AM. Cells were exposed to vehicle or 100 nM CN inhibitor CPM 20 min before measurement. Shown are means of biological individuals ($n > 45$, AUC: control = 100 ± 4.7%, CPM = 40.3 ± 5.7%, $p < 0.001$). *C,* insulin secretion of *INS1* 832/13 cells in response to 1.2 or 25 mM KCl with the presence of 3 mM glucose. Cells were exposed to CPM (100 nM) or vehicle 20 min before the experiment. Data are analyzed and represented as described in the legend to Fig. 2*A* ($n = 7$, *, $p < 0.05$; **, $p < 0.01$). *D,* SOCC-mediated cytosol Ca^{2+} influx in *INS1* 832/13 cells was measured using Fura2. Cells were exposed to the suggested chemicals 20 min before experiments. *E,* quantitative analysis of Fig. 6*D* based on AUC calculation. Data represent the percentage changes relative to WT control. Shown are mean ± S.E. ($n > 16$, *, $p < 0.05$; **, $p < 0.01$; ***, $p < 0.001$). *F,* SOCC-mediated cytosol Ca^{2+} influx in *INS1* 832/13 cells was measured using Fura2 following the procedure as described in the legend to Fig. 5*G*. Cells were exposed to the suggested chemicals 20 min before experiments ($n > 15$, AUC did not show significance between two treatments). *G,* SERCA-mediated ER Ca^{2+} refilling in *INS1* 832/13 cells was measured using the FRET-based D1ER probe following the same procedure as described in the legend to Fig. 5*B*. Cells were exposed to the indicated chemicals 20 min before experiments. *H,* quantitative analysis of Fig. 6*F* based on AUC measurement. Data represents as percentage changes relative to WT control. Shown are mean ± S.E. ($n > 5$, *, $p < 0.05$; **, $p < 0.01$).

($p < 0.05$) decrease in ER Ca^{2+} reuptake, whereas CGA brought ER Ca^{2+} reuptake in the PERK-inhibited cells back to control levels ($p < 0.05$). Taken together, the results were consistent with the hypothesis that PERK regulates Ca^{2+} signaling in a CN-dependent pathway.

DISCUSSION

Perk is among a small number of genes that are so important for maintaining glucose homeostasis that their loss results in permanent neonatal diabetes (43, 44), the most severe form of diabetes. Previously we showed that the diabetic phenotype of *Perk* genetic deficiency was due to the absence of PERK in pancreatic β-cells (19). However, the normal function of PERK in the β-cell has remained elusive. Initially it was proposed that the main function of PERK was to provide an adaptive response to presumed fluctuations in normal ER stress by temporarily repressing protein synthesis so as to ease client protein load in the ER (14, 16, 17). Subsequent studies on *Perk*-deficient mice and cultured β-cells, however, have generally not supported this hypothesis. Rather, we discovered dysfunctions in the basic

processes of the pancreatic β-cell including ablated glucose-stimulated insulin secretion (19, 27) and proinsulin trafficking (20). Because Ca^{2+} is a key driver of insulin granule exocytosis and PERK is activated by ER Ca^{2+} depletion, we postulated that these defects seen in GSIS could be due to misregulation of intracellular Ca^{2+}. The use of genetic tools to probe PERK function is confounded by compensatory adaptive responses that can obfuscate interpretations of underlying mechanisms. The development of a highly selective PERK inhibitor provided by GlaxoSmithKline (22) provided us a powerful tool to determine the immediate consequences of ablating PERK function. We found that acute inhibition of PERK enzymatic activity rapidly leads to a reduction in both glucose- and KCl-stimulated insulin secretion, thus recapitulating the defect in stimulated insulin secretion when *Perk* is genetically ablated. Moreover, PERK inhibition resulted in pronounced suppression of glucose- and KCl-stimulated Ca^{2+} influx in both rat and human primary β-cells. To provide an independent method to confirm that PERK regulates stimulated Ca^{2+} uptake in β-cells, we employed a genetic method to acutely knockdown PERK expression through the use of shRNA directed against the *Perk* mRNA. We found that KCl-stimulated Ca^{2+} influx was strongly suppressed in β-cells that were knocked down for PERK expression.

Glucose or KCl stimulation of β-cells induces a major influx of Ca^{2+} into the cytosol that occurs largely through the voltage-dependent Ca^{2+} channels, and therefore we anticipated that the negative effect of the PERKi on Ca^{2+} uptake was due to inhibition of the VDCCs. However, direct measurement of the VDCC-dependent Ca^{2+} current showed no impact of PERK inhibition. Other plasma membrane ion channels such as store-operated Ca^{2+} channels and transient receptor potential channels, are known to either conduct Ca^{2+} or to synergize VDCC by further enhancing depolarization (3, 11, 45–47). The SOCC and some of the key TRP channels (*e.g.* TRPM2) are inhibited by 2-APB (48, 49). We found that like PERKi, 2-APB significantly suppresses insulin secretion as well as KCl-induced cytosol Ca^{2+} entry. Moreover, co-treatment of 2-APB and PI does not further inhibit KCl-stimulated cytosol Ca^{2+} entry consistent with the hypothesis that they act through the same pathway. Therefore we postulate that PERK regulates Ca^{2+} entry via one or more 2-APB sensitive ion channels.

Inasmuch as SOCE is purported to be dependent upon ER Ca^{2+} release (50), we examined the impact of PERK inhibition on ER Ca^{2+} release and reuptake. We found that PERKi does not induce ER Ca^{2+} depletion nor does it influence Ca^{2+} release stimulated by inhibition of SERCA or activation of IP_3 receptor. However, restoration of ER Ca^{2+}, in the wake of ER Ca^{2+} depletion/release, is strongly impaired by PERK inhibition. Because restoring ER Ca^{2+} is largely dependent upon SERCA, we propose that PERK positively regulates SERCA activity under conditions of diminished ER Ca^{2+} when SERCA is maximally activated. This proposal is supported by previous studies that PERK is activated under conditions of low ER Ca^{2+} and repressed when ER Ca^{2+} is at its high steady-state level (31). Thus PERK may function to induce SERCA to a highly activated state when rapid restoration of ER Ca^{2+} is required during acetylcholine-stimulated insulin secretion or when the ER is acting to buffer Ca^{2+} influx into the cytoplasm during glucose-stimulated insulin secretion (4). PERK and SERCA are unique to multicellular eukaryotes and neither is present in yeast. We postulate that emergence of PERK during evolution was in response to the need to modulate SERCA activity *vis à vis* intracellular Ca^{2+} dynamics.

How PERK regulates glucose- and KCl-stimulated Ca^{2+} entry and SERCA activity is an intriguing question in light of the well known activity for PERK of modulating gene expression via the eIF2α pathway. Inasmuch as *Perk* deficiency and an *eIF2α* knock-in mutation of the regulatory phosphorylation site in mice both result in proinsulin trafficking defect and diabetes (19, 52), it is clear that at least some of the functions of PERK in β-cells are mediated by eIF2α phosphorylation. However, the speed at which acute PERK inhibition can negatively affect Ca^{2+} entry into the cytoplasm and restoration of ER Ca^{2+} argues against the involvement of the eIF2α-mediated pathway and its subsequent regulation of protein synthesis. Hence we turned toward examining the possibility that PERK may mediate Ca^{2+} regulation through interaction with calcineurin (14), a Ca^{2+}/calmodulin-dependent protein phosphatase. In addition to a multiplicity of functions in modulating Ca^{2+}/calmodulin-dependent processes in the cell, CN was more recently shown to bind to PERK and increase its activation (53). The CN-dependent activation of PERK was also shown to be enhanced by increased cytoplasmic Ca^{2+} levels. In pancreatic β-cells, we confirmed that KCl-induced Ca^{2+} uptake increased PERK activity. We discovered that the effects of inhibiting CN on intracellular Ca^{2+} signaling in β-cells recapitulated the effects seen in PERK-inhibited cells including blunting glucose and KCl-stimulated Ca^{2+} uptake, restoration of ER Ca^{2+}, and inhibition of SOCE. Moreover, hyperactivation of CN was able to significantly reverse the negative effects of PERKi on Ca^{2+} regulation, supporting the hypothesis that CN lies downstream of PERK in modulating intracellular Ca^{2+}. Because immunosuppression therapy using CN inhibitors often leads to diabetes, CN has been suspected of playing an important role in β-cell development and function (24). Recently a targeted mutation of the *calcineurin b1* (*Cnb1*) mouse gene has revealed that CN is required for normal insulin secretion, β-cell proliferation, and glucose homeostasis (25). Indeed, the postnatal diabetic progression in *Cn1b* KO mice closely mimics that of *Perk* KO mice.

We propose that PERK mediates its regulation of SERCA via a sequence of steps including PERK activation of CN, inactivation of calnexin, and release of calnexin inhibition of SERCA (Fig. 8). The restoration of ER Ca^{2+} as synergized by this pathway may be particularly important to non-nutrient secretagogues such as acetylcholine that act through the phospholipase C-IP_3 pathway. Stimulated release of ER Ca^{2+} stores via the IP_3 receptor not only helps to drive insulin secretion but also the resultant ER Ca^{2+} depletion further induces Ca^{2+} uptake through plasma membrane SOCC. Thus PERK- and CN-dependent regulation of SERCA and SOCC may also orchestrate non-nutrient secretagogue stimulation of insulin secretion.

The identities of the plasma membrane channels or receptors that mediate PERK- and CN-dependent regulation of Ca^{2+} uptake stimulated by glucose and KCl are as yet uncertain.

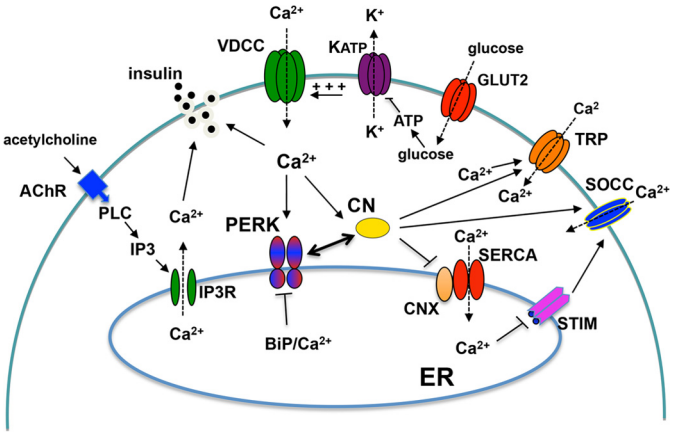

FIGURE 8. **Proposed model for regulation of Ca^{2+} dynamics in insulin secreting β-cells by PERK and calcineurin.** PERK activity may be directly regulated by cytoplasmic Ca^{2+} or indirectly through interaction with calcineurin, a known cytoplasmic Ca^{2+} sensor. In contrast Ca^{2+} depletion in the ER can result in PERK activation. PERK-dependent regulation of Ca^{2+} uptake in the ER is likely to be mediated through calcineurin dephosphorylation of calnexin and disassociation with SERCA. Release of CNX from SERCA then results in activation of SERCA and restoration of ER Ca^{2+}. SERCA plays an important role in buffering Ca^{2+} entering of the cytoplasmic during glucose-stimulated secretion and restoring ER Ca^{2+} following acetylcholine-stimulated insulin secretion. PERK and CN also act together to regulate plasma membrane channels and receptors such as TRP and SOCC to regulate glucose-stimulated Ca^{2+} entry into the cytoplasm.

Treatment of β-cells with glucose or KCl results in elevation rather than depletion of ER Ca^{2+}, and therefore participation of SOCE in the initial Ca^{2+} spike would seem unlikely because SOC is argued to be induced by ER Ca^{2+} depletion (50). However, we found that 2-APB, a potent inhibitor of SOCC (35), strongly blunts glucose- and KCl-stimulated Ca^{2+} uptake. We speculate that either SOCC is activated by the rapid increase in externally derived Ca^{2+} or that 2-APB blocks a channel or receptor that is activated by the rise in cytosolic Ca^{2+} conducted by the VDCC. The dependence of SOCC activation on ER Ca^{2+} depletion has been challenged, in part, by the finding that under physiological conditions the ER does not experience substantial Ca^{2+} depletion (54). In addition, SOCC has been shown to be sensitive to small changes in cytoplasmic Ca^{2+}. Further studies will be required to identify the factors regulated by PERK and CN, which modulate the rapid rise in cytoplasmic Ca^{2+} via the VDCC in response to glucose stimulation of β-cells.

Why PERK has evolved to regulate Ca^{2+} dynamics is likely tied to how PERK activity is regulated. Although others have proposed that PERK is primarily activated by the accumulation of unfolded proteins in the ER under stress conditions (55), we noted previously that PERK is normally activated in highly secretory tissues such as the pancreas and therefore likely to be activated by normal physiological processes (14, 18). In this study we discovered that elevation of cytosolic Ca^{2+}, as induced by KCl, stimulated PERK activation. This is in contrast to activation of PERK associated with ER Ca^{2+} depletion that occurs when SERCA is inhibited. However, it should be noted that ER Ca^{2+} depletion results in a transient increase in cytosolic Ca^{2+}, which may be the cause of PERK activation. Bollo and co-workers (53) have suggested that CN may act as a Ca^{2+} sensor between the cytoplasm and ER. We further speculate that PERK and CN may act together to monitor and coordinate the balance between cytoplasmic and ER Ca^{2+} levels, which is critically important in the regulation of stimulated insulin secretion.

The discovery that PERK regulates cellular Ca^{2+} dynamics may have profound implications to PERK function in other organs and tissues such as the nervous system where Ca^{2+} plays a dominant role in synaptic transmission (56). Interestingly, PERK and CN have been shown to be required for flexibility in hippocampal-dependent memory extinction in spatial memory tasks (51, 57), and we suggest that this function may be dependent upon PERK and CN modulation of intracellular Ca^{2+} dynamics.

Acknowledgments—We thank Dr. Richard Ordway and Dr. Fumiko Kawasaki for advice and technical assistance with the FRET-based Ca^{2+} imaging experiments. We thank Dr. Jeff Axten and Dr. Rakesh Kumar for providing the GSK414 PERK inhibitor and discussions about the effects of PERK inhibition. We thank the National Institutes of Health NIDDK-funded Integrated Islet Distribution Program (IIDP) at City of Hope for providing human pancreatic islets. We thank Cavener Lab members Elyse Munoz, Carrie Lewis, Jingjie Hu, and Siying Zhu for technical assistance and Dr. Fumihiko Urano, Dr. Christopher Newgard, Dr. Jun-Ichi Miyazaki, and Dr. Jonathan Lytton for providing experimental materials.

REFERENCES

1. Straub, S. G., and Sharp, G. W. (2002) Glucose-stimulated signaling pathways in biphasic insulin secretion. *Diabetes Metab. Res. Rev.* **18,** 451–463
2. Henquin, J. C. (2000) Triggering and amplifying pathways of regulation of insulin secretion by glucose. *Diabetes* **49,** 1751–1760
3. Uchida, K., and Tominaga, M. (2011) The role of thermosensitive TRP (transient receptor potential) channels in insulin secretion. *Endocr. J.* **58,** 1021–1028
4. Ravier, M. A., Daro, D., Roma, L. P., Jonas, J. C., Cheng-Xue, R., Schuit, F. C., and Gilon, P. (2011) Mechanisms of control of the free Ca^{2+} concentration in the endoplasmic reticulum of mouse pancreatic beta-cells. Interplay with cell metabolism and $[Ca^{2+}]_c$ and role of SERCA2b and SERCA3. *Diabetes* **60,** 2533–2545
5. Kono, T., Ahn, G., Moss, D. R., Gann, L., Zarain-Herzberg, A., Nishiki, Y., Fueger, P. T., Ogihara, T., and Evans-Molina, C. (2012) PPAR-γ activation restores pancreatic islet SERCA2 levels and prevents beta-cell dysfunction under conditions of hyperglycemic and cytokine stress. *Mol. Endocrinol.* **26,** 257–271
6. Evans-Molina, C., Robbins, R. D., Kono, T., Tersey, S. A., Vestermark, G. L., Nunemaker, C. S., Garmey, J. C., Deering, T. G., Keller, S. R., Maier, B., and Mirmira, R. G. (2009) Peroxisome proliferator-activated receptor γ activation restores islet function in diabetic mice through reduction of endoplasmic reticulum stress and maintenance of euchromatin structure. *Mol. Cell. Biol.* **29,** 2053–2067
7. Cardozo, A. K., Ortis, F., Storling, J., Feng, Y. M., Rasschaert, J., Tonnesen, M., Van Eylen, F., Mandrup-Poulsen, T., Herchuelz, A., and Eizirik, D. L. (2005) Cytokines downregulate the sarcoendoplasmic reticulum pump Ca^{2+} ATPase 2b and deplete endoplasmic reticulum Ca^{2+}, leading to induction of endoplasmic reticulum stress in pancreatic beta-cells. *Diabetes* **54,** 452–461
8. Chen, L., Koh, D. S., and Hille, B. (2003) Dynamics of calcium clearance in mouse pancreatic beta-cells. *Diabetes* **52,** 1723–1731
9. Ahrén, B. (2000) Autonomic regulation of islet hormone secretion. Implications for health and disease. *Diabetologia* **43,** 393–410
10. Gilon, P., and Henquin, J. C. (2001) Mechanisms and physiological significance of the cholinergic control of pancreatic beta-cell function. *Endocr. Rev.* **22,** 565–604

11. Liu, Y. J., and Gylfe, E. (1997) Store-operated Ca^{2+} entry in insulin-releasing pancreatic beta-cells. *Cell Calcium* **22,** 277–286
12. Delépine, M., Nicolino, M., Barrett, T., Golamaully, M., Lathrop, G. M., and Julier, C. (2000) EIF2AK3, encoding translation initiation factor 2-α kinase 3, is mutated in patients with Wolcott-Rallison syndrome. *Nat. Genet.* **25,** 406–409
13. Harding, H. P., Zeng, H., Zhang, Y., Jungries, R., Chung, P., Plesken, H., Sabatini, D. D., and Ron, D. (2001) Diabetes mellitus and exocrine pancreatic dysfunction in *perk*$^{-/-}$ mice reveals a role for translational control in secretory cell survival. *Mol. Cell* **7,** 1153–1163
14. Zhang, P., McGrath, B., Li, S., Frank, A., Zambito, F., Reinert, J., Gannon, M., Ma, K., McNaughton, K., and Cavener, D. R. (2002) The PERK eukaryotic initiation factor 2α kinase is required for the development of the skeletal system, postnatal growth, and the function and viability of the pancreas. *Mol. Cell. Biol.* **22,** 3864–3874
15. Shi, Y., Vattem, K. M., Sood, R., An, J., Liang, J., Stramm, L., and Wek, R. C. (1998) Identification and characterization of pancreatic eukaryotic initiation factor 2 α-subunit kinase, PEK, involved in translational control. *Mol. Cell. Biol.* **18,** 7499–7509
16. Harding, H. P., Zhang, Y., and Ron, D. (1999) Protein translation and folding are coupled by an endoplasmic-reticulum-resident kinase. *Nature* **397,** 271–274
17. Harding, H. P., Zhang, Y., Bertolotti, A., Zeng, H., and Ron, D. (2000) Perk is essential for translational regulation and cell survival during the unfolded protein response. *Mol. Cell* **5,** 897–904
18. Cavener, D. R., Gupta, S., and McGrath, B. C. (2010) PERK in beta cell biology and insulin biogenesis. *Trends Endocrinol. Metab.* **21,** 714–721
19. Zhang, W., Feng, D., Li, Y., Iida, K., McGrath, B., and Cavener, D. R. (2006) PERK EIF2AK3 control of pancreatic beta cell differentiation and proliferation is required for postnatal glucose homeostasis. *Cell Metab.* **4,** 491–497
20. Gupta, S., McGrath, B., and Cavener, D. R. (2010) PERK (EIF2AK3) regulates proinsulin trafficking and quality control in the secretory pathway. *Diabetes* **59,** 1937–1947
21. Senée, V., Vattem, K. M., Delépine, M., Rainbow, L. A., Haton, C., Lecoq, A., Shaw, N. J., Robert, J. J., Rooman, R., Diatloff-Zito, C., Michaud, J. L., Bin-Abbas, B., Taha, D., Zabel, B., Franceschini, P., Topaloglu, A. K., Lathrop, G. M., Barrett, T. G., Nicolino, M., Wek, R. C., and Julier, C. (2004) Wolcott-Rallison Syndrome. Clinical, genetic, and functional study of EIF2AK3 mutations and suggestion of genetic heterogeneity. *Diabetes* **53,** 1876–1883
22. Axten, J. M., Medina, J. R., Feng, Y., Shu, A., Romeril, S. P., Grant, S. W., Li, W. H., Heerding, D. A., Minthorn, E., Mencken, T., Atkins, C., Liu, Q., Rabindran, S., Kumar, R., Hong, X., Goetz, A., Stanley, T., Taylor, J. D., Sigethy, S. D., Tomberlin, G. H., Hassell, A. M., Kahler, K. M., Shewchuk, L. M., and Gampe, R. T. (2012) Discovery of 7-methyl-5-(1-{[3-(trifluoromethyl)phenyl]acetyl}-2,3-dihydro-1H-indol-5-yl)-7H-p yrrolo[2,3-d]pyrimidin-4-amine (GSK2606414), a potent and selective first-in-class inhibitor of protein kinase R (PKR)-like endoplasmic reticulum kinase (PERK). *J. Med. Chem.* **55,** 7193–7207
23. Atkins, C., Liu, Q., Minthorn, E., Zhang, S. Y., Figueroa, D. J., Moss, K., Stanley, T. B., Sanders, B., Goetz, A., Gaul, N., Choudhry, A. E., Alsaid, H., Jucker, B. M., Axten, J. M., and Kumar, R. (2013) Characterization of a novel PERK kinase inhibitor with anti-tumor and anti-angiogenic activity. *Cancer Res.*, **73,** 1993–2002
24. Heit, J. J. (2007) Calcineurin/NFAT signaling in the beta-cell. From diabetes to new therapeutics. *Bioessays* **29,** 1011–1021
25. Goodyer, W. R., Gu, X., Liu, Y., Bottino, R., Crabtree, G. R., and Kim, S. K. (2012) Neonatal beta cell development in mice and humans is regulated by calcineurin/NFAT. *Dev. Cell* **23,** 21–34
26. Bollo, M., Paredes, R. M., Holstein, D., Zheleznova, N., Camacho, P., and Lechleiter, J. D. (2010) Calcineurin interacts with PERK and dephosphorylates calnexin to relieve ER stress in mammals and frogs. *PloS One* **5,** e11925
27. Feng, D., Wei, J., Gupta, S., McGrath, B. C., and Cavener, D. R. (2009) Acute ablation of PERK results in ER dysfunctions followed by reduced insulin secretion and cell proliferation. *BMC Cell Biol.* **10,** 61
28. Kitamura, T., Kido, Y., Nef, S., Merenmies, J., Parada, L. F., and Accili, D. (2001) Preserved pancreatic beta-cell development and function in mice lacking the insulin receptor-related receptor. *Mol. Cell. Biol.* **21,** 5624–5630
29. Quesada, I., Tudurí, E., Ripoll, C., and Nadal, A. (2008) Physiology of the pancreatic alpha-cell and glucagon secretion. Role in glucose homeostasis and diabetes. *J. Endocrinol.* **199,** 5–19
30. Roe, M. W., Fiekers, J. F., Philipson, L. H., and Bindokas, V. P. (2006) Visualizing calcium signaling in cells by digitized wide-field and confocal fluorescent microscopy. *Methods Mol. Biol.* **319,** 37–66
31. Moore, C. E., Omikorede, O., Gomez, E., Willars, G. B., and Herbert, T. P. (2011) PERK activation at low glucose concentration is mediated by SERCA pump inhibition and confers preemptive cytoprotection to pancreatic beta-cells. *Mol. Endocrinol.* **25,** 315–326
32. Liang, S. H., Zhang, W., McGrath, B. C., Zhang, P., and Cavener, D. R. (2006) PERK (eIF2α kinase) is required to activate the stress-activated MAPKs and induce the expression of immediate-early genes upon disruption of ER calcium homoeostasis. *Biochem. J.* **393,** 201–209
33. Islam, M. S. (2010) Calcium signaling in the islets. *Adv. Exp. Med. Biol.* **654,** 235–259
34. Berridge, M. J. (2002) The endoplasmic reticulum. A multifunctional signaling organelle. *Cell Calcium* **32,** 235–249
35. Bootman, M. D., Collins, T. J., Mackenzie, L., Roderick, H. L., Berridge, M. J., and Peppiatt, C. M. (2002) 2-Aminoethoxydiphenyl borate (2-APB) is a reliable blocker of store-operated Ca^{2+} entry but an inconsistent inhibitor of $InsP_3$-induced Ca^{2+} release. *FASEB J.* **16,** 1145–1150
36. Bird, G. S., DeHaven, W. I., Smyth, J. T., and Putney, J. W., Jr. (2008) Methods for studying store-operated calcium entry. *Methods* **46,** 204–212
37. Palmer, A. E., Jin, C., Reed, J. C., and Tsien, R. Y. (2004) Bcl-2-mediated alterations in endoplasmic reticulum Ca^{2+} analyzed with an improved genetically encoded fluorescent sensor. *Proc. Natl. Acad. Sci. U.S.A.* **101,** 17404–17409
38. Roderick, H. L., Lechleiter, J. D., and Camacho, P. (2000) Cytosolic phosphorylation of calnexin controls intracellular Ca^{2+} oscillations via an interaction with SERCA2b. *J. Cell Biol.* **149,** 1235–1248
39. Turner, H., Gomez, M., McKenzie, E., Kirchem, A., Lennard, A., and Cantrell, D. A. (1998) Rac-1 regulates nuclear factor of activated T cells (NFAT) C1 nuclear translocation in response to Fcϵ receptor type 1 stimulation of mast cells. *J. Exp. Med.* **188,** 527–537
40. Hogan, P. G., Chen, L., Nardone, J., and Rao, A. (2003) Transcriptional regulation by calcium, calcineurin, and NFAT. *Genes Dev.* **17,** 2205–2232
41. Enan, E., and Matsumura, F. (1992) Specific inhibition of calcineurin by type II synthetic pyrethroid insecticides. *Biochem. Pharmacol.* **43,** 1777–1784
42. Tong, L., Song, Y., Jia, Z., Zhang, W., and Wei, Q. (2007) Calmodulin-dependent activation of calcineurin by chlorogenic acid. *IUBMB Life* **59,** 402–407
43. Aguilar-Bryan, L., and Bryan, J. (2008) Neonatal diabetes mellitus. *Endocr. Rev.* **29,** 265–291
44. Rubio-Cabezas, O., Patch, A. M., Minton, J. A., Flanagan, S. E., Edghill, E. L., Hussain, K., Balafrej, A., Deeb, A., Buchanan, C. R., Jefferson, I. G., Mutair, A., Neonatal Diabetes International Collaborative Group, Hattersley, A. T., and Ellard, S. (2009) Wolcott-Rallison syndrome is the most common genetic cause of permanent neonatal diabetes in consanguineous families. *J. Clin. Endocrinol. Metab.* **94,** 4162–4170
45. Dyachok, O., and Gylfe, E. (2001) Store-operated influx of Ca^{2+} in pancreatic beta-cells exhibits graded dependence on the filling of the endoplasmic reticulum. *J. Cell Sci.* **114,** 2179–2186
46. Tamarina, N. A., Kuznetsov, A., and Philipson, L. H. (2008) Reversible translocation of EYFP-tagged STIM1 is coupled to calcium influx in insulin secreting beta-cells. *Cell Calcium* **44,** 533–544
47. Jacobson, D. A., and Philipson, L. H. (2007) TRP channels of the pancreatic beta cell. *Handb. Exp. Pharmacol.* **179,** 409–424
48. Thore, S., Dyachok, O., Gylfe, E., and Tengholm, A. (2005) Feedback activation of phospholipase C via intracellular mobilization and store-operated influx of Ca^{2+} in insulin-secreting beta-cells. *J. Cell Sci.* **118,** 4463–4471

49. Togashi, K., Inada, H., and Tominaga, M. (2008) Inhibition of the transient receptor potential cation channel TRPM2 by 2-aminoethoxydiphenyl borate (2-APB). *Br. J. Pharmacol.* **153,** 1324–1330
50. Putney, J. W., Jr. (1986) A model for receptor-regulated calcium entry. *Cell Calcium* **7,** 1–12
51. Trinh, M. A., Kaphzan, H., Wek, R. C., Pierre, P., Cavener, D. R., and Klann, E. (2012) Brain-specific disruption of the eIF2α kinase PERK decreases ATF4 expression and impairs behavioral flexibility. *Cell Rep.* **1,** 676–688
52. Scheuner, D., Song, B., McEwen, E., Liu, C., Laybutt, R., Gillespie, P., Saunders, T., Bonner-Weir, S., and Kaufman, R. J. (2001) Translational control is required for the unfolded protein response and *in vivo* glucose homeostasis. *Mol. Cell* **7,** 1165–1176
53. Bollo, M., Paredes, R. M., Holstein, D., Zheleznova, N., Camacho, P., and Lechleiter, J. D. (2010) Calcineurin interacts with PERK and dephosphorylates calnexin to relieve ER stress in mammals and frogs. *PLoS One* **5,** e11925
54. Gill, D. L., and Patterson, R. L. (2004) Toward a consensus on the operation of receptor-induced calcium entry signals. *Sci. STKE* 2004, pe39
55. Bertolotti, A., Zhang, Y., Hendershot, L. M., Harding, H. P., and Ron, D. (2000) Dynamic interaction of BiP and ER stress transducers in the unfolded-protein response. *Nat. Cell. Biol.* **2,** 326–332
56. Llinás, R., Steinberg, I. Z., and Walton, K. (1981) Relationship between presynaptic calcium current and postsynaptic potential in squid giant synapse. *Biophys. J.* **33,** 323–351
57. Shaw, J. A., Matlovich, N., Rushlow, W., Cain, P., and Rajakumar, N. (2012) Role of calcineurin in inhibiting disadvantageous associations. *Neuroscience* **203,** 144–152